



Synthesis and evaluation of [¹¹C]Cimbi-806 as a potential PET ligand for 5-HT₇ receptor imaging

Matthias M. Herth^{a,b,c,†}, Hanne D. Hansen^{a,†}, Anders Ettrup^a, Agnete Dyssegaard^a, Szabolcs Lehel^c, Jesper Kristensen^b, Gitte M. Knudsen^{a,*}

^a Center for Integrated Molecular Brain Imaging, Rigshospitalet and University of Copenhagen, Blegdamsvej 9, DK-2100 Copenhagen, Denmark

^b Institute for Medicinal Chemistry, The Faculty of Pharmaceutical Sciences, University of Copenhagen, Universitetsparken 2, DK-2100 Copenhagen, Denmark

^c PET and Cyclotron Unit, Rigshospitalet, Blegdamsvej 9, DK-2100 Copenhagen, Denmark

ARTICLE INFO

Article history:

Received 1 February 2012

Revised 6 April 2012

Accepted 3 May 2012

Available online 18 May 2012

Keywords:

[¹¹C]2-(2',6'-dimethoxy-[1,1'-biphenyl]-3-yl)-N,N-dimethylethanamine

5-HT₇ receptor

PET

[¹¹C]Cimbi-806

ABSTRACT

2-(2',6'-Dimethoxy-[1,1'-biphenyl]-3-yl)-N,N-dimethylethanamine has been identified as a potent ligand for the serotonin 7 (5-HT₇) receptor. In this study, we describe the synthesis, radiolabeling and in vivo evaluation of [¹¹C]2-(2',6'-dimethoxy-[1,1'-biphenyl]-3-yl)-N,N-dimethylethanamine ([¹¹C]Cimbi-806) as a radioligand for imaging brain 5-HT₇ receptors with positron emission tomography (PET). Precursor and reference compound was synthesized and subsequent ¹¹C-labelling with [¹¹C]methyltriflate produced [¹¹C]Cimbi-806 in specific activities ranging from 50 to 300 GBq/μmol. Following intravenous injection, brain uptake and distribution of [¹¹C]Cimbi-806 was assessed with PET in Danish Landrace pigs. The time–activity curves revealed high brain uptake in thalamic and striatal regions (SUV ~2.5) and kinetic modeling resulted in distribution volumes (V_T) ranging from 6 mL/cm³ in the cerebellum to 12 mL/cm³ in the thalamus. Pretreatment with the 5-HT₇ receptor antagonist SB-269970 did not result in any significant changes in [¹¹C]Cimbi-806 binding in any of the analyzed regions. Despite the high brain uptake and relevant distribution pattern, the absence of appropriate in vivo blocking with a 5-HT₇ receptor selective compounds renders the conclusion that [¹¹C]Cimbi-806 is not an appropriate PET radioligand for imaging the 5-HT₇ receptor in vivo.

© 2012 Elsevier Ltd. All rights reserved.

1. Introduction

The brain serotonin (5-HT) system is known to be involved in various central nervous system (CNS) disorders, for example, depression,¹ and drugs with pharmacological effects on the 5-HT system are among the most frequently used for brain disorders. The most recently discovered receptor in the 5-HT receptor family, the 5-HT₇ receptor, is also considered associated with depression. The atypical antipsychotic drug amisulpride has antidepressive effects^{2,3} and studies in 5-HT₇ receptor knock-out mice support that the 5-HT₇ receptor antagonism of amisulpride causes this effect.⁴ Other atypical antipsychotics also have relative high affinity for the 5-HT₇ receptor although their direct involvement in alleviating depressive symptoms through 5-HT₇ antagonism remains to be investigated.^{5,6} Furthermore, there is also evidence that the 5-HT₇ receptor is involved in psychosis, circadian rhythm, and sleep architecture (for review see⁷).

* Corresponding author. Tel.: +45 3545 6720; fax: +45 3545 6713.

E-mail address: gmk@nru.dk (G.M. Knudsen).

† Both authors have contributed equally.

In vivo studies of cerebral 5-HT₇ receptor binding in humans would provide a significant advance in the understanding of the above mentioned physiology and pathophysiology. Positron emission tomography (PET) is used to non-invasively quantify neuroreceptor binding in vivo and the availability of an appropriate PET radiotracer for the 5-HT₇ receptor would be of particular interest. Previous attempts to develop a 5-HT₇ receptor PET radioligand have been made but unfortunately so far with limited success.^{8,9} Most recently, an ¹⁸F-labeled SB-269970 derivative was synthesized and evaluated^{10,11} but in this study the arterial input function was not determined and in the absence of a valid reference region, the 5-HT₇ receptor selectivity in vivo of this PET radioligand still remains to be determined.

In the past years, several lead structures of 5-HT₇ receptor binding ligands have been identified within different structural classes.¹² Among these lead structures, biphenethylamines represent an easy moiety for both organic synthesis and radiochemical labelling and in addition has an interesting selectivity profile.^{13,14} Especially, 2-(2',6'-dimethoxy-[1,1'-biphenyl]-3-yl)-N,N-dimethylethanamine (Cimbi-806) is of interest, because of its simple synthesis and its favorable dissociation constant (K_i) for the 5-HT₇ receptor (K_i = 8.6 nM) over the 5-HT_{1A} receptor (K_i = 4826 nM).¹³ This large

difference in K_i is necessary because of the relative low 5-HT₇ receptor density (B_{\max}) in the brain and also because 5-HT₇ and 5-HT_{1A} receptors are located in similar brain regions, such as the hippocampus and cortical areas.^{15,16} Based on the literature values,^{15,16} one can compute that in order to ensure that less than 10% PET signal from the 5-HT_{1A} receptors, a selectivity of at least 350-fold (based on B_{\max} values in relevant regions) is required for specific imaging the cerebral 5-HT₇ receptor binding.

In this study, we synthesized the precursor for [¹¹C]Cimbi-806 radiolabelling and subsequently evaluated its in vivo brain uptake and binding characteristics in the pig.

2. Results and discussion

2.1. Organic chemistry

Bisphenylethylamines were synthesized a similar manner as previously described.¹³ The method involves formation of 2,6-dimethoxybenzeneboronic acid (**4**) and bromoethylamine derivatives, which were consequently reacted via Suzuki-cross-coupling to form the bisphenylethylamine matrix of [¹¹C]Cimbi-806. The Suzuki reaction was performed in good yields (>80%) under inert conditions in a microwave in 2–4 h. Reaction times of the cross-coupling varied and therefore, the completion of reaction was checked by thin layer chromatography. However, conventional heating for 12 h lead mainly to the reduced phenethylamine derivative rather than the bisphenylethylamine. Syntheses of precursor and reference compound of Cimbi-806 are summarized in Scheme 1.

To minimize synthesis efforts, both precursor and the reference compound of [¹¹C]Cimbi-806 was produced in an one-reaction sequence. Thus, 3-bromophenethylamine was not directly bismethylated, but Boc-protected which resulted in an almost complete conversion. 2,6-dimethoxybenzeneboronic acid (**4**) was synthesized in moderate yields (~30%) by lithiating 1,3-dimethoxybenzene and then reacting with B(OMe)₃. Afterwards, the Boc-protected derivative (**1**) and the boronic acid (**4**) were cross-coupled in excellent yields (~90%).

Several unsuccessful attempts were made to synthesize the precursor (**6**) from this cross-coupled intermediate (**5**). Reduction of the carbamate to the mono-methylated secondary amine with 4 equiv of LiAlH failed and only trace amounts of the precursor (**6**) could be detected via gas chromatography. In addition, methylation of (**5**) by activating the amine with NaH and reacting with MeI followed by TFA Boc-deprotecting only resulted in primary amine (**8**), probably since the alkylation was hindered by the Boc-group. However, Boc-deprotection of (**5**) leads to yields close to 80% and consequently reductive alkylation with aqueous formaldehyde resulted in the reference compound (Cimbi-806) in excellent yields (~80%).

Two strategies were applied to synthesize the precursor: Mono-methylated bromophenylethylamine was produced starting either by reacting 3-bromophenethylbromide with aqueous methylamine in a condensation reaction or by nosylation and methylation of 3-bromophenethylamine in a one-pot reaction. The condensation reaction only resulted in poor amounts (~10%) of (**2**) even when different bases or varying temperatures were applied. However, the Nosyl-protection followed by base activated methylation with MeI resulted in complete conversion to (**3**).

Cross-coupling of (**2**) and (**3**) with 2,6-dimethoxybenzeneboronic acid (**4**) under microwave yielded in the precursor (**6**) or the intermediate (**7**) (~80–90%). The following thiolysis of (**7**) to the precursor (**6**) succeeded in 52% without any attempts to optimize this deprotection step, such as using higher concentration of thiol groups or increasing the reaction temperature. We isolated (**6**) in sufficient amounts for labelling purposes as well as for synthesising Cimbi-806 via reductive alkylation. Taken together, the

precursor (**6**) and the reference compound of [¹¹C]Cimbi-806 were synthesized in sufficient amounts in overall chemical yields of 43% and 28%, respectively.

2.2. Lipophilicity

The lipophilicities of promising compounds were determined using the HPLC method according to Krass et al.¹⁷ The logD of Cimbi-806 was determined to be 4.4. This value may appear a little high compared to the optimal logD interval for small molecules to penetrate the blood–brain-barrier (BBB) as suggested by Rowley et al.¹⁸ to be 2–3. But in our set-up other known CNS-PET ligands (e.g., MDL 100907, altanserin or WAY 100635) show similar high values. This fact gives rise to the assumption that [¹¹C]Cimbi-806 may have similarly good properties for molecular imaging.

2.3. In vitro autoradiography

The in vitro dissociation constant (K_i) for Cimbi-806 displacement of [³H]SB-269970 binding on pig brain sections was 8.82 ± 0.04 nM (Fig. 1), in accordance with the previously reported K_i -value.¹³ The displacement of [³H]SB-269970 by Cimbi-806 was encouraging for in vivo PET experiments.

2.4. Radiochemistry

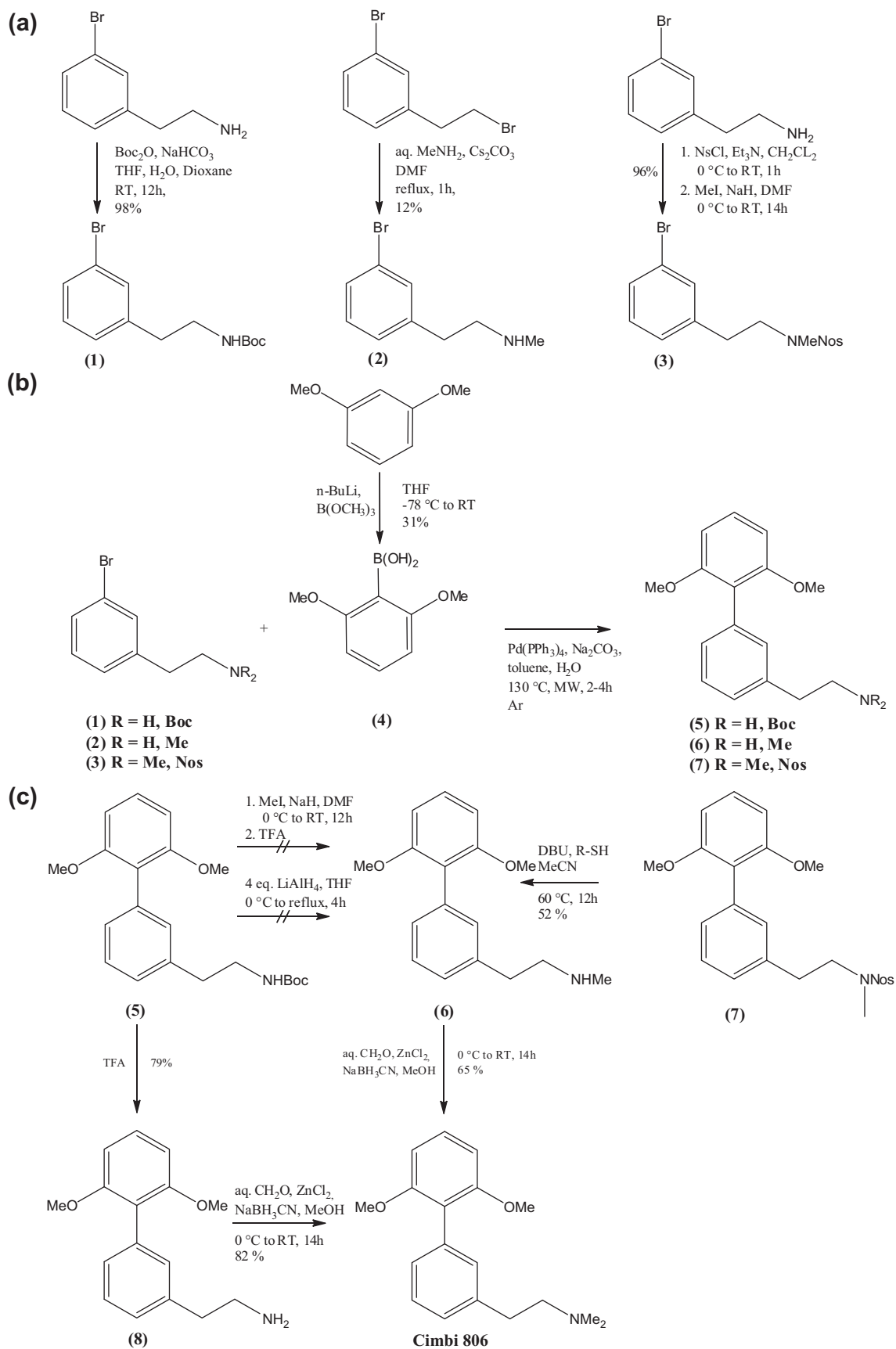
Radiolabeling of [¹¹C]Cimbi-806 (Scheme 2) using only 0.3 mg precursor (**6**) and [¹¹C]CH₃OTf was done with a fully automated system (RCY ~95%).¹⁹ [¹¹C]Cimbi-806 at ~400 s was the only radioactive peak that was observed. Precursor (**6**) eluted 80 s prior to the radiolabelled product as indicated by the UV-absorption (data not shown). The radiosynthesis including HPLC purification and formulation generated an injectable solution of [¹¹C]Cimbi-806 (radiochemical purity >96%) within 80–90 min. Typically, 0.6–1.8 GBq of [¹¹C]Cimbi-806 was isolated with a specific activities (A_s) of 50–300 GBq/μmol at end of synthesis.

2.5. In vivo PET imaging

After intravenous injection of [¹¹C]Cimbi-806, a rapid and high uptake in the pig brain was observed (Fig. 2). Time-activity curves (TACs) and summed PET images show highest [¹¹C]Cimbi-806 uptake in the thalamus and the striatum and lowest uptake in the cerebellum. The TACs showed reversible kinetics of [¹¹C]Cimbi-806 with peak SUV at ~20 min followed by a relative fast decline in tissue activity.

With the high uptake of Cimbi-806 as seen in these experiments, the relatively high lipophilicity value for Cimbi-806 does not seem to be a problem. This outcome also holds true for many other CNS-PET ligands (e.g., MDL 100907, altanserin, and WAY 100635) where high values are determined, but the tracers have good brain uptake.

To investigate the selectivity of [¹¹C]Cimbi-806 in vivo, blocking experiments was performed in three pigs after the baseline scan. Pre-treatment followed by continuous infusion throughout the scan with 0.5 or 1.0 mg/kg/h of SB-269970 did not result in any significant changes in [¹¹C]Cimbi-806 distribution volumes. Contrary to the expected displacement, and increased uptake of [¹¹C]Cimbi-806 was observed in the thalamus, as seen on the TACs (Fig. 2B). This effect was only observed in the thalamus region and not in any other region investigated. All metabolite corrected plasma input functions were analyzed but no significant changes were observed in input function between baseline and blocked (SB-269970) conditions. The difference in uptake cannot be ascribed to blocking of peripheral 5-HT₇ receptor sites by the SB-269970 compound.



Scheme 1. Chemical syntheses: (a) Synthesis of 3-bromophenethylamine derivatives (b) Synthesis route for the biphenyl core (c) Synthesis of precursor and reference compound of [^{11}C]Cimbi-806.

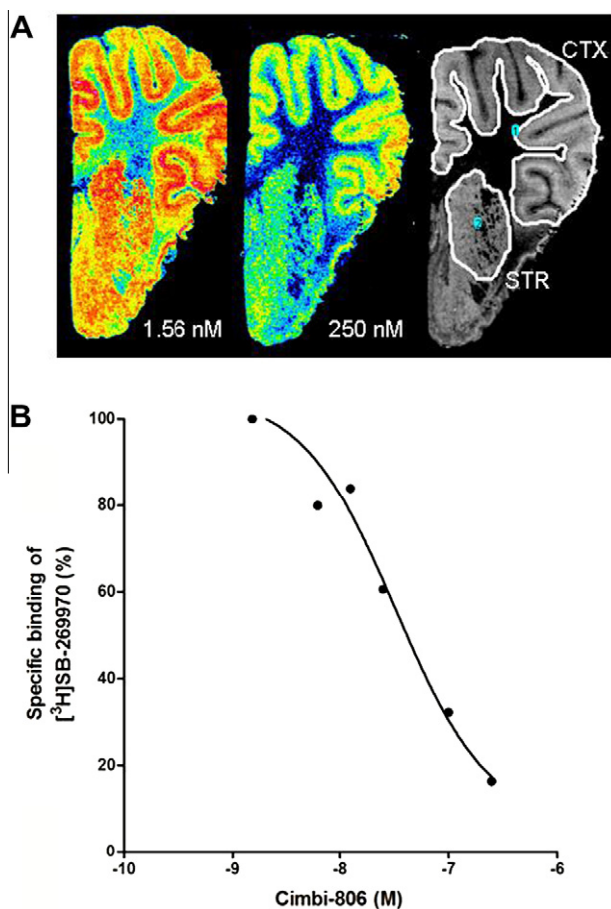


Figure 1. (A) In vitro competition autoradiography images with [³H]SB-269970 and two concentrations of **Cimbi-806** (left: 1.56 nM, right: 250 nM). (B) Inhibition of [³H]SB-269970 binding to pig brain sections by **Cimbi-806**.

In all pigs, full arterial plasma parent compound input curves were measured and these were used to calculate the distribution volumes (V_T) of [¹¹C]Cimbi-806 in volumes of interest (VOIs) using a one-tissue compartment (1-TC) model. An averaged metabolite curve (based on seven separate injections) was used to correct plasma activity for parent compound fraction as previously described²⁰

No significant changes in V_T after SB-269970 pre-treatment was found in any region ($P > 0.5$, 2-way analysis of variance (ANOVA), Bonferroni post-test) (Fig. 3). High similarity between the deduced amino acid sequences of human and pig 5-HT₇ receptors²¹ and a pharmacokinetic study confirming BBB penetration of SB-269970

in rat,²² makes it unlikely that the lack of blockade in this study is caused by insufficient BBB penetration of the blocking agent. Thus, since it was not displaced by the selective compound SB-269970, we could not determine if [¹¹C]Cimbi-806 in vivo binding is selective for the 5-HT₇ receptor. The lack of displacement by SB-269970 could also be due to the radioligand having non-target affinity or because of high non-specific binding in the brain.

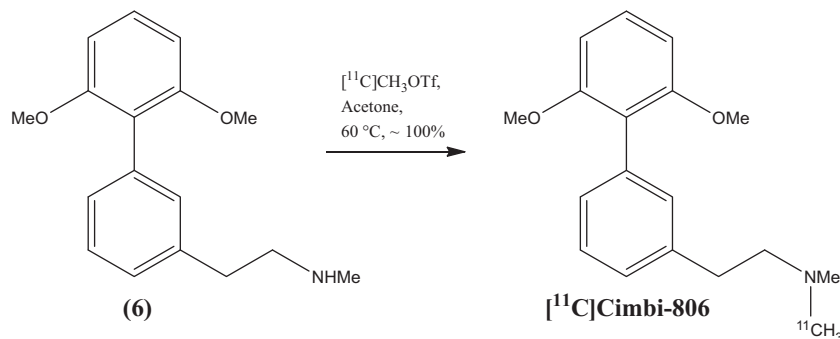
An autoradiographic study with [³H]SB-269970 to visualize the distribution of 5-HT₇ receptors in human whole hemisphere brain sections found that binding was mainly found in the thalamus, hypothalamus and hippocampal formation of the human brain,¹⁶ which was in good agreement with autoradiographic studies carried out on rat and guinea-pig brain sections.^{23,24} However differences were found when looking at the striatum, where the 5-HT₇ selective radioligand [³H]SB-269970 shows low binding and the less selective radioligand [³H]mesulergine found high binding.²⁵ The autoradiographic experiments carried out on pig brain sections in this study showed high binding in the cortical areas but also relatively high binding in the striatum (Fig. 1A). With this in mind we expect high binding of [¹¹C]Cimbi-806 in the thalamus and medium binding in the striatum and cortex. Binding in the cerebellum is expected, as 5-HT₇ receptors have been found in pig cerebellum.²¹ V_T values were indeed higher in thalamus and striatum and lower in the cerebellum (Fig. 3). Compared to human data, high striatal binding was not expected but as seen on the autoradiographic images it is likely that a higher density of 5-HT₇ receptors can be found in the pig striatum, and thereby accounting for the unexpected high uptake of [¹¹C]Cimbi-806.

2.6. In vivo metabolism of [¹¹C]Cimbi-806

After intravenous injection, [¹¹C]Cimbi-806 was rapidly metabolized (Fig. 4) and this generated two radiolabelled metabolites that both were less lipophilic than [¹¹C]Cimbi-806. The parent compound fraction at baseline and pre-treatment conditions, showed no significant difference, indicating that pretreatment with SB-269970 did not affect [¹¹C]Cimbi-806 metabolism. The free fraction of [¹¹C]Cimbi-806 in plasma (f_p) was $23.5 \pm 5.0\%$ (mean \pm SD, $n = 10$) after 3 h when equilibrium between the dialysis chambers was reached.

3. Conclusion

Cimbi-806 and its desmethyl precursor were synthesized in sufficient yields, and ¹¹C-radiolabeling produced [¹¹C]Cimbi-806 in high specific radioactivity, high radiochemical purity and yield. Evaluation of [¹¹C]Cimbi-806 in pigs with PET scanning revealed high brain uptake, and appropriate radiometabolism with only two polar metabolites, unlikely to cross the BBB, appearing in pig plasma. Since [¹¹C]Cimbi-806 could not be displaced by the



Scheme 2. Radiosynthesis of [¹¹C]Cimbi-806.

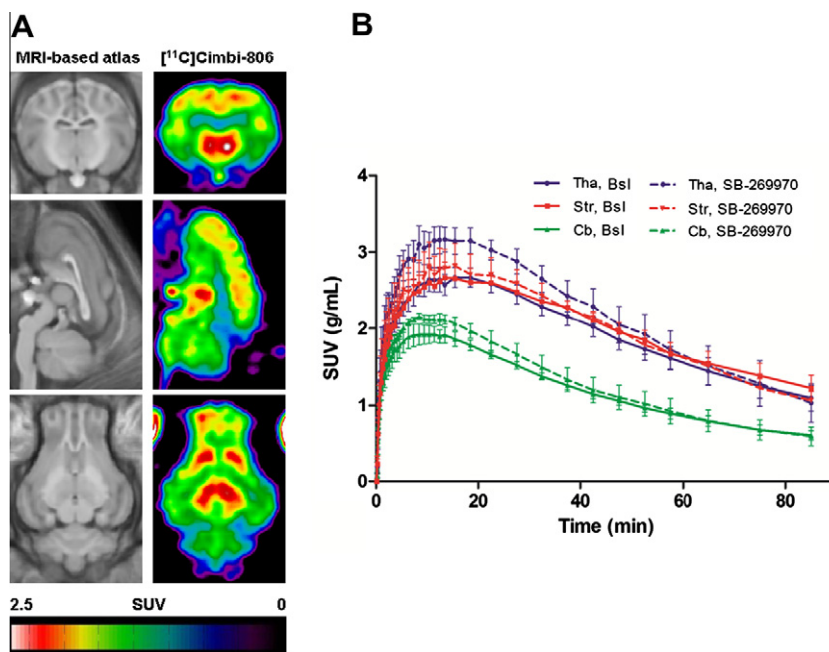


Figure 2. (A) Representative PET images summed from 0 to 90 min scanning showing regional uptake of $[^{11}\text{C}]\text{Cimbi-806}$ (right column) and the standardized MRI-based atlas for the pig brain to which the PET images are co-registered (left column). (B) Time-activity curves at baseline (solid lines, $n = 5$) and blocked (dashed lines, $n = 3$) conditions. Bsl = baseline, Tha = thalamus, Str = striatum, Cb = Cerebellum, TACs are represented as standardized uptake value (SUV) \pm S.E.M.

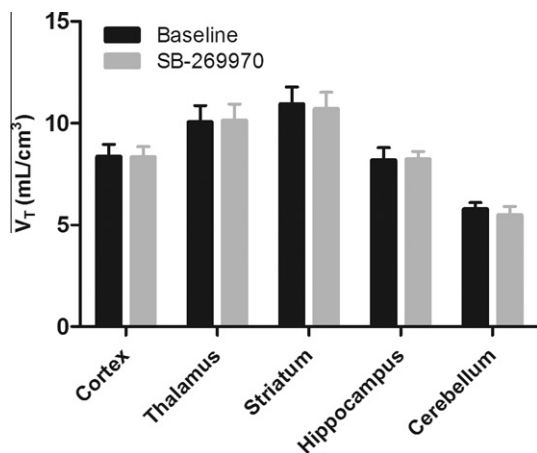


Figure 3. Distribution volumes (V_T) of $[^{11}\text{C}]\text{Cimbi-806}$. Mean \pm S.E.M. distribution volumes for one-tissue compartment (1TC) modeling of baseline ($n = 4$) and blocked ($n = 3$) for the different brain regions.

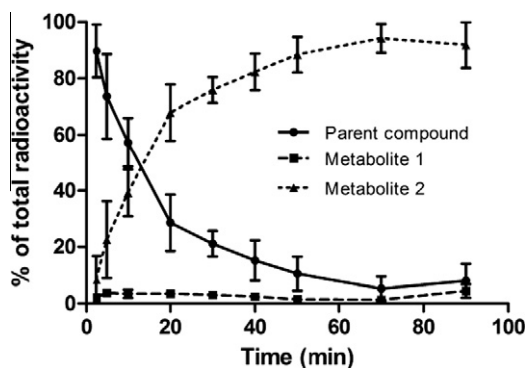


Figure 4. $[^{11}\text{C}]\text{Cimbi-806}$ (solid line) and metabolites (dashed lines) as a function of time after intravenous injection. The graph shows the average of measurements from seven experiments, error bars represent S.D.

selective 5-HT₇ receptor antagonist SB-269970 in vivo, we do not find this PET radioligand to be suitable for imaging the 5-HT₇ receptor.

4. Experimental details

4.1. Chemicals and equipment

Chemicals were purchased from Acros, Fluka, Sigma, Tocris, ABX or Merck. Unless otherwise stated, all chemicals were used without further purification. $[^3\text{H}]\text{SB-269970}$ was purchased from PerkinElmer. Microwave-assisted synthesis was carried out in a Biotage Initiator apparatus operating in single mode; the microwave cavity producing controlled irradiation at 2.45 GHz (Biotage AB, Uppsala, Sweden). The reactions were run in sealed vessels (0.5–2.0 mL). These experiments were performed by employing magnetic stirring and a fixed hold time using variable power to reach (during 1–2 min) and then maintain the desired temperature in the vessel for the programmed time period. The temperature was monitored by an IR sensor focused on a point on the reactor vial glass. The IR sensor was calibrated to internal solution reaction temperature by the manufacturer. GC–MS were performed on a Shimadzu. For Solid Phase Extraction (SPE), Sep-Pak[®]-C18-cartridges (Waters, USA) were used. Thin Layer Chromatography (TLC) was performed using plates from Merck (Silicagel 60 F254 and Alumina oxide 60 F254). $^1\text{H-NMR}$ spectra were recorded using a Bruker AC 300 spectrometer. Chemical shifts are quoted as δ -values (ppm) downfield from tetramethylsilane (TMS). Field desorption (FD) mass spectra were recorded using a Finnigan MAT90 spectrometer. Analytical and preparative high performance liquid chromatography (HPLC) were performed on a Dionex system consisting of a pump P680A pump, a UVD 170U detector and a Scansys radiodetector. Metabolite analysis of pig plasma was performed using a Dionex Ultimate 3000 HPLC system consisting of a DGP-3600SD pump and an online Posi-Ram Radio Flow-Through Detector. Brain slices were cut on a HM5000M Cryostat (Microm Intl GmbH). Fuji imaging plates (IP) were scanned by a Fuji BAS-2500 scanner. PET scanning was

performed with a high-resolution research tomography scanner (HRRT, Siemens AG). [^{13}C]Methane was produced via the $^{14}\text{N}(\text{p},\alpha)^{11}\text{C}$ reaction by bombardment of an [^{14}N]N $_2$ containing 10% H $_2$ target with a 17 MeV proton beam in a Scanditronix MC32NI cyclotron.

4.2. Organic synthesis

4.2.1. [2-(3-Bromo-phenyl)-ethyl]-carbamic acid *tert*-butyl ester (1)

To a solution of 3-bromophenethylamine (3.12 g, 15.7 mmol) and NaHCO $_3$ (2.3 g, 27.38 mmol) in THF (50 mL), H $_2$ O (50 mL) and dioxane (50 mL) were added (Boc) $_2$ O (4.1 g, 18.8 mmol). This mixture was stirred for 12 h and then extracted with CH $_2$ Cl $_2$. The combined organic layers were dried, filtered and evaporated to yield **1** (4.66 g 98%) as a colorless liquid. ^1H NMR (300 MHz, CDCl $_3$): δ 7.30–7.27 (m, 2H, ArH), 7.11–7.07 (m, 2H, ArH), 3.30 (q, J = 6 Hz, 2H, NCH $_2$), 2.72 (t, J = 9 Hz, 2H, ArCH $_2$), 1.40 (s, 9H, *tert*-butyl); TLC R $_f$: 0.52 (Heptane/EtOAc 3:1) (full analytical data are reported in²⁶).

4.2.2. 2-(3-Bromophenyl)-*N*-methylethanamine (2)

To a solution of 3-bromophenethylbromide (1 g, 3.83 mmol) in DMF (10 mL) was added 40% aqueous methylamine (2.97 mL, 38.3 mmol), followed by Cs $_2$ CO $_3$ (1.625 g, 5 mmol). After the reaction mixture was refluxed for 1 h, it was cooled to room temperature and the solvent was removed. The residue was dissolved in ethyl acetate (30 mL), and the organic layer was washed with water (3 \times 20 mL) and dried over Na $_2$ SO $_4$. The solvent was removed in vacuo, and the oily residue was further purified using flash column chromatography (CHCl $_3$ /MeOH 5:2) yielding in **2** (100 mg, 12%) as a colorless liquid. ^1H NMR (300 MHz, CDCl $_3$): δ 7.26–7.23 (m, 2H, ArH), 7.06–7.04 (m, 2H, ArH), 2.78–2.74 (m, 4H), 2.30 (s, 3H, NCH $_3$); TLC R $_f$: 0.2 (CHCl $_3$ /MeOH 5:2); GC–MS (EI) m/z (% rel Int.): 214 (100.0 [M] $^+$), rt: 7.240 min (full analytical data are reported in²⁷).

4.2.3. *N*-(3-Bromophenethyl)-*N*-methyl-2-nitrobenzenesulfonamide (3)

2-(3-Bromophenyl)ethanamine (2 g, 10.05 mmol) were dissolved in anhydrous CH $_2$ Cl $_2$ (50 mL) and Et $_3$ N (2 g, 20 mmol, 2.77 mL) and cooled to 0 °C. 2-nosylchloride (2.21 g, 10 mmol) was added dropwise and the mixture was warmed to rt and stirred for 1 h. The mixture was diluted with Et $_2$ O, quenched with 10% aq HCl and washed successively with sat. NaHCO $_3$ and brine. After drying with Na $_2$ SO $_4$, the solvent was evaporated to yield 3.8 g of crude product (~100%) which was used without any further purification and dissolved in DMF (10 mL). NaH (60% dispersion in mineral oil, 397.2 mg, 10 mmol) and after 15 min, Mel (0.91 g, 5.28 mmol, 0.4 mL) were added at 0 °C. The mixture was stirred at room temperature for 14 h, hereafter, DMF was removed. The resultant mixture was diluted in a mixture of EtOAc/H $_2$ O and extracted with ethyl acetate three times. The combined organic layers were dried over Na $_2$ SO $_4$ and concentrated. The residue was purified by flash chromatography on silica gel with EtOAc/Heptane (2:1) yielding in **3** (3.87 g, 96%) as a yellowish liquid. ^1H NMR (300 MHz, CDCl $_3$): δ 7.95–7.92 (m, 1H, ArH), 7.70–7.60 (m, 3H, ArH), 7.37–7.27 (m, 2H, ArH), 7.19–7.11 (m, 2H, ArH), 3.51–3.46 (m, 2H, NCH $_2$), 2.99–2.87 (m, 5H, NCH $_3$ and ArCH $_2$); ^{13}C NMR (75 MHz, CDCl $_3$): δ 148.15, 140.49, 133.84, 132.47, 132.00, 131.93, 130.80, 130.43, 130.01, 127.79, 124.36, 122.71, 51.81, 35.32, 34.69; TLC R $_f$: 0.8 (Heptane/EtOAc 2:1); GC–MS (EI) m/z (% rel Int.): 398.0 (100.0 [M] $^+$), rt: 22.298 min.

4.2.4. 2,6-Dimethoxybenzeneboronic acid (4)

2,6-Dimethoxybenzeneboronic acid was synthesized as reported.²⁸

4.2.5. General procedure for the Suzuki cross-coupling

The appropriate phenylbromide (0.517 mmol), 2,6-dimethoxybenzeneboronic acid (170 mg, 0.9 mmol) and Na $_2$ CO $_3$ (137.65 mg, 1.29 mmol) were dissolved in a mixture of toluene/H $_2$ O (10:1) (5.5 mL) and sparged with argon for at least 30 min to assure all oxygen is removed from the reaction mixture. Pd(PPh $_3$) $_4$ (29.86 mg, 0.026 mmol) were added and heated for 2–4 h in a microwave oven (Initiator, Biotage) at 130 °C. The resulting reaction mixture was quenched with water and extracted by diethylether. After drying with MgSO $_4$ the united organic layers were reduced and the crude mixture was purified by column chromatography yielding in the desired product.

4.2.6. *tert*-Butyl 2-(2',6'-dimethoxy-[1,1'-biphenyl]-3-yl)ethyl carbamate (5)

Colorless liquid (173 mg 94%); ^1H NMR (300 MHz, CDCl $_3$): δ 7.30–7.12 (m, 5H, ArH), 6.67–7.07 (d, J = 9 Hz 2H, ArH), 3.75 (s, 6H, OCH $_3$), 3.45 (q, J = 6 Hz 2H, NCH $_2$), 2.85 (t, J = 9 Hz 2H, ArCH $_2$), 1.48 (s, 9H, *tert*-butyl); ^{13}C NMR (75 MHz, CDCl $_3$): δ 157.72, 156.04, 138.27, 134.41, 131.61, 129.17, 128.88, 128.15, 127.45, 119.44, 104.39, 79.44, 56.29, 42.00, 35.47, 28.84; TLC R $_f$: 0.31 (Heptane/EtOAc 3:1); GC–MS (EI) m/z (% rel Int.): 357 (100.0 [M] $^+$), rt: 16.307 min.

4.2.7. 2-(2',6'-Dimethoxy-[1,1'-biphenyl]-3-yl)-*N*-methyl-ethanamine (6)

Colorless liquid (116 mg; 83%); ^1H NMR (300 MHz, CDCl $_3$): δ 7.31–7.14 (m, 5H, ArH), 6.63 (d, J = 6 Hz 2H, ArH), 3.71 (s, 6H, OCH $_3$), 2.89–2.81 (m, 4H, ArCH $_2$ CH $_2$ N), 2.43 (s, 3H, NCH $_3$), 1.64 (br s, 1H, NH); TLC R $_f$: 0.15 (EtOAc/Et $_3$ N 3:1); GC–MS: 271 g/mol, rt: 12.806 min, purity: 100% (full analytical data are reported in²⁹).

4.2.8. *N*-(2-(2',6'-Dimethoxy-[1,1'-biphenyl]-3-yl)ethyl)-*N*-methyl-2-nitrobenzenesulfonamide (7)

White solide (205 mg; 87%); mp: 128–129 °C; ^1H NMR (300 MHz, CDCl $_3$): δ 7.90–7.87 (m, 1H, ArH), 7.63–7.54 (m, 3H, ArH), 7.28–7.26 (m, 2H, ArH), 7.20–7.17 (m, 2H, ArH), 7.11–7.09 (m, 1H, ArH), 6.63 (d, J = 9 Hz 2H, ArH), 3.71 (s, 6H, OCH $_3$), 3.49 (t, J = 9 Hz, 2H, NCH $_2$), 2.95–2.90 (m, 5H, NCH $_3$ and ArCH $_2$); ^{13}C NMR (75 MHz, CDCl $_3$): δ 157.73, 137.32, 134.66, 133.48, 132.84, 131.74, 131.64, 130.95, 129.48, 128.94, 128.14, 127.41, 125.58, 124.18, 119.33, 104.40, 56.23, 56.13, 35.36, 35.29; TLC R $_f$: 0.5 (Heptane/EtOAc 1:1).

4.2.9. 2-(2',6'-Dimethoxy-[1,1'-biphenyl]-3-yl)-*N*-methylethanamine (6)

A 10 mL round-bottom flask was charged with 1-dodecylmercaptan (0.722 g, 3.57 mmol, 0.854 mL) and acetonitrile (25 mL). The mixture is cooled in an ice-water bath and of DBU (0.542 g, 3.57 mmol, 0.533 mL) was added over a period of 10 min. After 5 min, the ice-water bath was removed, and **7** (791 mg, 1.785 mmol) in acetonitrile (20 mL) is added and the mixture was heated to 60 °C for 12 h. The crude mixture was taken up in EtOAc and washed with Na $_2$ CO $_3$ and dried over MgSO $_4$, filtered, and concentrated under reduced pressure. The residue was purified by column chromatography on silica. First the column was flushed with (Heptane/EtOAc 1:1) to remove all byproducts and then with EtOAc/Et $_3$ N (2:0.3) to yield the desired secondary amine as a colorless oil (250 mg, 52%). (See above for analytical data)

4.2.10. 2-(2',6'-Dimethoxy-[1,1'-biphenyl]-3-yl)ethanamine (8)

Compound **5** (0.105 mg, 0.294 mm) were carefully dissolved in TFA (5 mL). The resulting mixture was stirred for 4 h. Afterwards, TFA was removed in vacuo and the resulting mixture solved in diethylether. Then the pH was set to 8 by addition of 1 M NaHCO $_3$ and then extracted with diethylether (3 \times). After drying with

Na₂SO₄ the united organic layers were reduced to yield in the desired product (60 mg, 79%) as a colorless liquid. ¹H NMR (300 MHz, CDCl₃): δ 7.34–7.10 (m, 5H, ArH), 6.50 (d, *J* = 6 Hz, 2H, ArH), 4.79 (br s, 2H, NH₂), 3.71 (s, 6H, OCH₃), 3.04 (t, *J* = 6 Hz, 2H, NCH₂), 2.87 (t, *J* = 6 Hz, 2H, ArCH₂); ¹³C NMR (75 MHz CDCl₃): δ 157.67, 138.01, 134.50, 131.64, 129.33, 128.93, 128.17, 127.51, 111.34, 104.40, 56.18, 42.89, 38.16; TLC R_f: 0.01 (Heptane/EtOAc 3:1); GC–MS (EI) *m/z* (% rel Int.): 257 (100.0 [M]⁺), rt 12.467 min.

4.2.11. General procedure to synthesize 2-(2',6'-dimethoxy-[1,1'-biphenyl]-3-yl)-N,N-dimethylethanamine (Cimbi-806)

To a stirred solution of the appropriate amine (1.32 mmol), zinc chloride (90 mg, 0.65 mmol), and 37% aqueous formaldehyde (0.4 mL, 5.28 mmol) in MeOH (10 mL) was added sodium cyanoborohydride (99.64 mg, 1.584 mmol) at 0 °C. The resulting mixture was stirred at room temperature for 14 h and then quenched by addition of 1 N NaOH and extracted with ethyl acetate. The combined organic layers were dried over Na₂SO₄ and concentrated. The residue was purified by flash chromatography on silica gel with EtOAc/Et₃N (10:0.1) to yield in a colorless oil. Method A: Starting from **6** resulting in Cimbi-806 (244 mg, 65%). Method B: Starting from **8** resulting in the desired product (319 mg, 82%). ¹H NMR (300 MHz, CDCl₃): δ 7.36–7.25 (m, 2H, ArH), 7.20–7.18 (m, 3H, ArH), 6.65 (d, *J* = 6 Hz, 2H, ArH), 3.74 (s, 6H, OCH₃), 2.87–2.81 (m, 2H, NH₂), 2.64–2.58 (m, 2H, ArCH₂), 2.32 (s, 6H, NCH₃); ¹³C NMR (75 MHz, CDCl₃): δ 157.99, 139.67, 134.39, 131.67, 129.00, 128.99, 128.09, 127.54, 104.57, 99.38; 61.93, 56.30, 44.61, 34.88; TLC R_f: 0.2 (Heptane/Et₃N 10:0.1); GC–MS (EI) *m/z* (% rel Int.): 285 (100.0 [M]⁺), rt: 11.513 min, purity: >99%.

4.3. Radiolabeling of [¹¹C]Cimbi-806

¹¹C-methyl trifluoromethanesulfonate ([¹¹C]MeOTf) produced using a fully automated system was transferred in a stream of helium to a 1.1-mL vial containing the labeling precursor **6** (0.3–0.4 mg) and acetone (300 μL). The resulting mixture was heated at 60 °C for 180 s and then purified by HPLC on a Luna 5 μm C18(2) 100 Å column (Phenomenex Inc.) (250 × 10 mm; 25:75 acetonitrile: 0.1% phosphoric acid; and flow rate, 6 mL/min, retention times: [¹¹C]Cimbi-806 = 7 min; precursor (**6**) = 5.4 min). The fraction corresponding to the labeled product (11.5 min) was collected in sterile water (150 mL), and the resulting solution was passed through a solid-phase C18 Sep-Pak extraction column (Waters Corp.), which had been preconditioned with ethanol (10 mL), followed by isotonic sodium chloride solution (20 mL). The column was flushed with sterile water (3 mL). Then, the trapped radioactivity was eluted with ethanol (3 mL), followed by isotonic sodium chloride solution (3 mL) into a 20-mL vial containing phosphate buffer (9 mL, 100 mM, pH 7), giving a 15 mL solution of [¹¹C]Cimbi-806 with a pH of approximately 7. In a total synthesis time of 80–90 min, 0.6–1.8 GBq of [¹¹C]Cimbi-806 was produced.

4.3.1. Determination of radiochemical purity and specific radioactivity

The radiotracer preparation was visually inspected for clarity, and absence of color and particles. Chemical and radiochemical purities were assessed on the same aliquot by HPLC analysis. Specific activity (A_s) of the radiotracers were calculated from three consecutive HPLC analyses (average) and determined by the area of the UV absorbance peak corresponding to the radiolabeled product on the HPLC chromatogram and compared to a standard curve relating mass to UV absorbance (λ = 225 μm). Column used for [¹¹C]Cimbi-806: Luna 5 μm C18(2) 100 Å column (Phenomenex Inc.) (150 × 4.6 mm (25:75 acetonitrile: 0.1% phosphoric acid; and flow rate: 2 mL/min, retention times: [¹¹C]Cimbi-806 = 2.618 min; precursor (**6**) = 2.247 min).

4.4. Lipophilicity

Lipophilicities were determined using a Dionex Ultimate 3000 HPLC equipped with de-gasser, autosampler, column-oven and UV-detector. The eluent was 50:50 (v/v) 25 mM sodium phosphate-buffer (pH = 7.4) and MeOH. Injected volumes were 100 μL with a flow rate of 2 mL/min. The column was a Zorbax SB-C8 (250 mm × 4.6 mm, 5 μm). The column oven was kept at 37 °C and detection was at 254 nm. The logarithm of retention factor of reference compounds (phenol, acetophenone, *p*-cresol, benzene, toluene, chlorobenzene, benzophenone, naphthalene, diphenyl and phenanthrene) and tested compounds was calculated, and a plot of the reference values against their known log *D* values was used to calculate log *D* values for tested compounds.

4.5. Animal procedures

Five female Danish Landrace pigs were used in this study (weight 19 kg). After arrival, animals were housed under standard conditions and were allowed to acclimatize for one week before scanning. To minimize stress, the animals were provided with straw bedding and environment enrichment, in the form of plastic balls and metal chains. On the scanning day, pigs were tranquilized by intramuscular (im) injection of 0.5 mg/kg midazolam. Anesthesia was induced by im injection of a Zoletil veterinary mixture (1.25 mg/kg tiletamin, 1.25 mg/kg zolazepam, and 0.5 mg/kg midazolam; Virbac Animal Health, France). Following induction, anesthesia was maintained by intravenous (iv) infusion of 15 mg/kg/h propofol (B. Braun Melsugen AG). During anesthesia, animals were endotracheally intubated and ventilated (volume 250 mL, frequency 16 per min). Venous access was granted through two catheters (Becton Dickinson) in the peripheral milk veins, and an arterial line for blood sampling measurement was obtained by a catheter in the femoral artery after a minor incision. Vital signs including blood pressure and heart rate were monitored throughout the duration of the PET scanning. Immediately after scanning, animals were sacrificed by iv injection of pentobarbital/lidocain. All animal procedures were approved by the Danish Council for Animal Ethics (Journal No. 2007/561-1320).

4.6. PET scanning protocol

[¹¹C]Cimbi-806 (*n* = 7) was given as intravenous bolus injections, and the pigs were subsequently PET-scanned for 90 min in list mode with the HRRT scanner. Scanning began at the time of injection. After the baseline scan, pigs were maintained in anesthesia and scanned a second time using the same PET-protocol. The 5-HT₇ antagonist, SB-269970 was administered 30 min prior to the second scan (0.5–1.0 mg/kg/h infusion). Infusion was continued for the remaining of the scan. An average of 468 ± 31 MBq was injected of [¹¹C]Cimbi-806, the average specific activity at the time of injection was 123 GBq/μmol (range: 30–215 GBq/μmol), and the average mass injected 1.6 μg (range: 0.61–4.3 μg). During the first 30 min of scanning, radioactivity in whole blood was continuously measured using an ABSS autosampler (Allog Technology) counting coincidences in a lead-shielded detector. Concurrently, blood samples were manually drawn at 2.5, 5, 10, 20, 30, 40, 50, 70, and 90 min and the radioactivity in whole blood was measured using a well counter (Cobra 5003, Packard Instruments) that was cross-calibrated to the HRRT scanner and autosampler.

4.7. Quantification of PET data

90-minute HRRT list-mode PET data were reconstructed into 38 dynamic frames of increasing length (6 × 10, 6 × 20, 4 × 30, 9 × 60, 2 × 180, 8 × 300, and 3 × 600 s). Images consisted of 207 planes and 256 × 256 voxels of 1.22 × 1.22 × 1.22 mm. A summed

picture of all counts in the 90-min scan was reconstructed for each pig and used for co-registration to a standardized MRI-based atlas of the Danish Landrace pig brain, similar to that previously published.^{30,31} The temporal radioactivity in volumes of interest (VOIs), including the cerebellum, cortex, hippocampus, lateral and medial thalamus, caudate nucleus, and putamen, was extracted. Activity in the striatum was averaged over the caudate nucleus and putamen. Activity in the thalamus was averaged over the lateral and medial thalamus. Radioactivity in all VOIs was calculated as the average of radioactive concentration (Bq/mL) in the left and right sides. Outcome measure in the time-activity curves was calculated as radioactive concentration in VOI (in kBq/mL) normalized to the injected dose corrected for animal weight (in kBq/kg), yielding standardized uptake values (SUV, in the unit of g/mL).

In all pigs, full arterial function was measured. A population-based averaged metabolite curve of the seven scans was constructed and subsequently used to correct plasma activity in the individual scans for parent compound fraction. We calculated the distribution values (V_T) VOIs for [¹¹C]Cimbi-806 using plasma corrected for parent compound as arterial input function. The one-tissue compartment (1TC) model was chosen for quantitative analysis the data Kinetic modeling was done with PMOD software (version 3.0; PMOD Technologies Inc.).

4.8. HPLC analysis of pig plasma

[¹¹C]Cimbi-806 was separated from its radio-labelled metabolite(s) by direct injection of plasma in a column switching HPLC system. Whole blood samples were centrifuged (3500 rpm, 7 min) and the supernatant plasma fraction was collected and filtered through a 0.45 μm syringe filter prior to analysis with online radioactive detection, as previously described.³²

4.9. Protein binding

The free fraction of [¹¹C]Cimbi-806 in plasma, f_p , was estimated using an equilibrium dialysis chamber method as previously described.³¹ Briefly, the dialysis was conducted in chambers (Harvard Biosciences) separated by cellulose membrane with a protein cut-off of 10,000 Da. Small amounts of [¹¹C]Cimbi-806 (~5 MBq) were added to 5 mL plasma sample from the pig. Plasma (500 μL) was then dialyzed at 37 °C against an equal volume of buffer (135 mM NaCl, 3.0 mM KCl, 1.2 mM CaCl₂, 1.0 mM MgCl₂, and 2.0 mM KH₂PO₄, pH 7.4). Counts per minute in 400 μL of plasma and buffer were determined in a well counter after various dialysis times, and f_p of [¹¹C]Cimbi-806 was calculated as the ratio of radioactivity in buffer and plasma. The samples were measured after equilibrium had been obtained between the two chambers.

4.10. In vitro autoradiography

Twenty micrometers coronal sections of pig brain (weight ~19 kg) were cut on a HM5000M Cryostat (Microm Intl GmbH) and thawed-mounted on super frost plus glass slides, air-dried and stored at –80 °C until use. Sections were cut so both cortical and striatal areas were visible. Autoradiography was performed with 5 nM [³H]SB-269970 (PerkinElmer, Inc.) and with increasing competing concentrations of Cimbi-806 (1.56–250 nM). Non-specific binding was determined with 5 μM SB-258719 (Tocris Bioscience). Two separate experiments were carried out on adjacent sections from the same pig. Assay buffer used consistend of 50 mM Tris–HCl, pH 7.4, and an incubation time of 2 h was used. Sections were washed 3 × 5 min in ice-cold assay buffer with a subsequent dip in ice-cold dH₂O. Sections were dried and exposed to Fujifilm tritium-sensitive imaging plates for 14 days. Specific radioligand binding (total minus non-specific binding) was plotted as a function

of concentration of Cimbi-806 and regressed using Prism 4.0 software to obtain K_i .

Acknowledgments

The authors wish to thank the staff at the PET and Cyclotron unit for expert technical assistance. We also want to thank Mette Værum Olesen and Letty Klarskov for excellent animal preparation as well as Lasse Kofoed Bech for logD measurements. Financial support by Intra European Fellowship (MC-IEF-275329), The Faculty of Health, University of Copenhagen, and the Lundbeck Foundation is gratefully acknowledged. The John & Birthe Meyer Foundation and The Toyota foundation are acknowledged for granting the HRRT scanner and the HPLC system, respectively.

A. Supplementary data

Supplementary data associated with this article can be found, in the online version, at <http://dx.doi.org/10.1016/j.bmc.2012.05.005>.

References and notes

- Carr, G. V.; Lucki, I. *Psychopharmacology (Berl)* **2011**, *213*, 265.
- Cassano, G. B.; Jori, M. C. *Int. Clin. Psychopharmacol.* **2002**, *17*, 27.
- Lecrubier, Y.; Boyer, P.; Turjanski, S.; Rein, W. J. *Affect. Disord.* **1997**, *43*, 95.
- Abbas, A. I.; Hedlund, P. B.; Huang, X. P.; Tran, T. B.; Meltzer, H. Y.; Roth, B. L. *Psychopharmacology (Berl)* **2009**, *205*, 119.
- Ishibashi, T.; Horisawa, T.; Tokuda, K.; Ishiyama, T.; Ogasa, M.; Tagashira, R.; Matsumoto, K.; Nishikawa, H.; Ueda, Y.; Toma, S.; Oki, H.; Tanno, N.; Saji, I.; Ito, A.; Ohno, Y.; Nakamura, M. *J. Pharmacol. Exp. Ther.* **2010**, *334*, 171.
- Smith, C.; Rahman, T.; Toohey, N.; Mazurkiewicz, J.; Herrick-Davis, K.; Teitler, M. *Mol. Pharmacol.* **2006**, *70*, 1264.
- Matthys, A.; Haegeman, G.; Van Craenenbroeck, K.; Vanhoenacker, P. *Mol. Neurobiol.* **2011**, *43*, 228.
- Zhang, M. R.; Haradahira, T.; Maeda, J.; Okauchi, T.; Kida, T.; Obayashi, S. *J. Labelled Compd. Radiopharm.* **2002**, *45*, 857.
- Andries, J.; Lemoine, L.; Mouchel-Blaisot, A.; Tang, S.; Verdurand, M.; Le, B. D.; Zimmer, L.; Billard, T. *Bioorg. Med. Chem. Lett.* **2010**, *20*, 3730.
- Lemoine, L.; Becker, G.; Vacher, B.; Billard, T.; Lancelot, S.; Newman-Tancredi, A.; Zimmer, L. *J. Nucl. Med.* **2011**, *52*, 1811.
- Andries, J.; Lemoine, L.; Le Bars, D.; Zimmer, L.; Billard, T. *Eur. J. Med. Chem.* **2011**, *46*, 3455.
- Leopoldo, M.; Lacivita, E.; Berardi, F.; Perrone, R.; Hedlund, P. B. *Pharmacol Ther* **2011**, *129*, 120.
- Paillet-Loilier, M.; Fabis, F.; Lepailleur, A.; Bureau, R.; Butt-Gueulle, S.; Dauphin, F.; Lesnard, A.; Delarue, C.; Vaudry, H.; Rault, S. *Bioorg. Med. Chem. Lett.* **2007**, *17*, 3018.
- Badarau, E.; Bugno, R.; Suzenet, F.; Bojarski, A. J.; Finaru, A. L.; Guillaumet, G. *Bioorg. Med. Chem.* **1958**, *2010*, 18.
- Hall, H.; Lundkvist, C.; Halldin, C.; Farde, L.; Pike, V. W.; McCarron, J. A.; Fletcher, A.; Cliffe, I. A.; Barf, T.; Wikstrom, H.; Sedvall, G. *Brain Res.* **1997**, *745*, 96.
- Varnas, K.; Thomas, D. R.; Tupala, E.; Tiitonen, J.; Hall, H. *Neurosci. Lett.* **2004**, *367*, 313.
- Krass, J. D.; Jastorff, B.; Genieser, H. G. *Anal. Chem.* **1997**, *69*, 2575.
- Rowley, M.; Kulagowski, J. J.; Watt, A. P.; Rathbone, D.; Stevenson, G. I.; Carling, R. W.; Baker, R.; Marshall, G. R.; Kemp, J. A.; Foster, A. C.; Grimwood, S.; Hargreaves, R.; Hurley, C.; Saywell, K. L.; Tricklebank, M. D.; Leeson, P. D. *J. Med. Chem.* **1997**, *40*, 4053.
- Jewett, D. M. *Int. J. Rad. Appl. Instrum. A* **1992**, *43*, 1383.
- Ettrup, A.; Mikkelsen, J. D.; Lehel, S.; Madsen, J.; Nielsen, E. O.; Palner, M.; Timmermann, D. B.; Peters, D.; Knudsen, G. M. *J. Nucl. Med.* **2011**, *52*, 1449.
- Bhalla, P.; Saxena, P. R.; Sharma, H. S. *Mol. Cell Biochem.* **2002**, *238*, 81.
- Hagan, J. J.; Price, G. W.; Jeffrey, P.; Deeks, N. J.; Stean, T.; Piper, D.; Smith, M. I.; Upton, N.; Medhurst, A. D.; Middlemiss, D. N.; Riley, G. J.; Lovell, P. J.; Bromidge, S. M.; Thomas, D. R. *Br. J. Pharmacol.* **2000**, *130*, 539.
- Gustafson, E. L.; Durkin, M. M.; Bard, J. A.; Zgombick, J.; Branchek, T. A. *Br. J. Pharmacol.* **1996**, *117*, 657.
- To, Z. P.; Bonhaus, D. W.; Eglén, R. M.; Jakeman, L. B. *Br. J. Pharmacol.* **1995**, *115*, 107.
- Martin-Cora, F. J.; Pazos, A. *Br. J. Pharmacol.* **2004**, *141*, 92.
- Broo, A.; Holm, P.; Judkins, R.; Li, L.; Lindstedt-Alstermark, E.-L.; Sandberg, P.; Swanson, M.; Weidolf, L.; Brickmann, K.; Patent number: EP1838687 (A1); 2006.
- Cheshire, D.; Cladingboel, D.; Hirst, S.; Manners, C.; Stocks, M. **2001**.
- Fukuda, T.; Sudo, E.-I.; Shimokawa, K.; Iwao, M. *Tetrahedron* **2008**, *64*, 328.
- Romero Alonso, L.; Zamanillo Castanedo, D.; Vela Hernández, J. M.; Buschmann, H. H.; Patent number EP1997493; 2008.
- Ettrup, A.; Palner, M.; Gillings, N.; Santini, M. A.; Hansen, M.; Rasmussen, L. K.; Nägren, K.; Madsen, J.; Begtrup, M.; Knudsen, G. M. *J. Nucl. Med.* **2010**, *51*, 1763.
- Kornum, B. R.; Lind, N. M.; Gillings, N.; Marner, L.; Andersen, F.; Knudsen, G. M. *J. Cereb. Blood Flow Metab.* **2009**, *29*, 186.
- Gillings, N. *Nucl. Med. Biol.* **2009**, *36*, 961.